Journal of Electronic Materials, Vol. 20, No. 12, 1991

Photoluminescence Excitation Spectroscopy of $InAs_{0.67}P_{0.33}$/InP Strained Single Quantum Wells

R. P. SCHNEIDER, JR.[1] and B. W. WESSELS

Department of Materials Science and Engineering and Materials Research Center, Northwestern University, Evanston, IL 60208

The optical emission characteristics of biaxially compressed $InAs_xP_{1-x}$/InP strained single quantum well (QW) structures, with nominal composition $x = 0.67$, have been investigated using photoluminescence (PL) and photoluminescence excitation (PLE) spectroscopies. The highly strained QWs exhibit intense and narrow PL in the 0.9–1.5 μm wavelength range, similar to the lattice-matched InGaAs(P)/InP system. The 20 K PLE spectra exhibit well-resolved features attributed to $n = 1$ heavy hole (E1H1) and light hole (E1L1) transitions in the 1.0–1.5 μm wavelength range. In addition, features attributed to transitions between $n = 2$ electrons and heavy holes (E2H2), and between $n = 1$ electrons and unconfined holes (E1Hf), were observed. The energy splitting between the heavy-hole and light-hole bands was found to be a sensitive measure of the band offsets in the system. The best prediction of this splitting was obtained for a valence band offset of $\Delta E_V \sim 0.25\Delta E_G$. This value of band offset was in agreement with the energy position of the E1Hf transition. The observed transition energies were also compared with the results of a finite square well model, taking into account the effects of strain, and the results offer further support for the band offset assignment. This study indicates that the InAsP system may be advantageous for application in strained-layer optoelectronic devices operating in the 1.3–1.6 μm wavelength range.

Key words: Photoluminescence, photoluminescence excitation, strained quantum wells, OMVPE, InGaAsP

INTRODUCTION

Strained-layer quantum well (QW) structures have received increasing attention for application to optoelectronic devices, particularly QW lasers.[1–4] The primary motivation for this work is the strain-induced modification of the in-plane valence band dispersion,[5] resulting in a reduction in such loss mechanisms as intervalence band absorption and nonradiative Auger recombination.[6–8] For devices operating in the 1.3–1.6 μm wavelength range, the lattice-matched InGaAs(P)/InP systems have received much attention, however recent theoretical and experimental work has focused on the development of strained-layer systems for such application.[2,4,7,9–12]

Recently the preparation of an alternative strained-layer QW system, $InAs_xP_{1-x}$/InP, has been investigated[13–15] because of its potential for 1.3–1.6 μm optoelectronic device application. QW structures exhibiting very intense and narrow photoluminescent (PL) emission and atomically smooth interfaces were prepared over the composition range $x \sim 0.4$–0.67. For a nominal composition of $x \sim 0.67$, and well thicknesses from 2 monolayers (ML)-8 nm, alloy bandgaps in the range 0.9–1.5 μm have been obtained, similar to the lattice-matched InGaAs(P)/InP QWs. However the strain in the InAsP wells is as large as ~2%, which should be advantageous for optoelectronic device applications. Preliminary characterization of these structures using PL indicated that the conduction band offset in the structures is about $0.7\Delta E_G$ (450 meV). This value is significantly greater than that found in the lattice-matched InGaAs(P) systems (310–370 meV, or 0.5–$0.6\Delta E_G$),[16–20] which should result in comparatively smaller hetero-barrier carrier leakage.[2] Furthermore, the corresponding valence band offset is 190 meV, very close to the minimum acceptable value of ~200 meV proposed in a recent theoretical treatment of the design parameters for long-wavelength strained-layer lasers.[7] These properties indicate that the InAsP/InP strained-layer QW system has significant potential for long-wavelength optoelectronic device applications.

To date, the photoluminescent properties of the InAsP/InP QW structures have been studied in some detail. However, a detailed study of the higher-energy excitonic transitions (*i.e.*, the light hole and $n = 2$ transitions) in $InAs_xP_{1-x}$ QWs has not yet been reported. Such a study is required to better characterize the band structure of the QW structures, especially the effect of strain and quantum confinement on the exciton energies, as well as to obtain a more reliable estimate for the band offsets. The band structure of several strained-layer QW systems has been described as a function of structural parameters using a similar analysis.[11,21,22]

In the present study, we have used photoluminescence excitation spectroscopy (PLE) to characterize the higher-energy excitonic transitions in highly strained $InAs_xP_{1-x}$/InP QW structures with

[1]Present address: Sandia National Laboratories, Division 1311, Albuquerque, NM, 87185-5800

0361-5235/1991/1401-1117$5.00©91 TMS

a nominal composition of $x = 0.67$ and well thicknesses of 1.2–4.5 nm. The samples used for this work are well-characterized, as has been reported previously,[13,14] and exhibit atomically smooth interfaces. The energy positions of the PLE peaks were compared with the predictions of a finite square well model, taking into account the effects of strain on the band structure. This analysis yields a more complete description of the band structure of the QWs, allowing a direct comparison of this system with lattice-matched InGaAs/InP and a better evaluation of the suitability of InAsP/InP QWs for similar optoelectronic device applications.

EXPERIMENTAL

The growth of the samples has been described in detail elsewhere.[13] The samples consisted of 1 to 4 $InAs_xP_{1-x}$ QWs of thickness 2 ML-8 nm, with a nominal well composition of $x \sim 0.67$, separated by 60 nm-thick InP barriers. The growth conditions for all of the samples was nominally the same, however slight differences in the growth rate were noted. The well thicknesses for each sample were calibrated against each other by comparing the PL peak energies. The composition of the wells was initially determined by measuring the emission energy of an 8 nm-thick QW, and correcting for small shifts due to quantum confinement and strain. The dependence of emission energy on well thickness for all of the samples was very similar, indicating that they are all of the same composition.

For the PLE setup, the excitation source consisted of the light from a 250 W tungsten-halogen lamp, filtered through a 0.25 m spectrometer with appropriate filters to eliminate interference from visible wavelengths. The light was focussed onto the sample, cooled to 20 K, in a rectangular (slit)-shaped spot, approximately 0.7 mm × 1.5 mm. The luminescence was collected and focussed into a Zeiss double-prism monochromator, set at the wavelength of the specified PL peak. Detection was with a liquid N_2-cooled North Coast Ge detector, and standard lock-in techniques were used for signal analysis. All of the spectra were corrected for the system response.

RESULTS AND DISCUSSION

The PL spectra from two multiple-SQW samples used for this work are given in Fig. 1. For each of the structures, 4 QWs were grown with the thicknesses indicated in the figure. Several sharp PL peaks are observed to originate from each of the wells in the structures, and the peak energies in the two structures overlap. These spectra are treated in greater detail elsewhere.[14] The peak splitting noted in the spectra corresponds to emission from extended regions in the QW which are atomically smooth, and which differ in thickness by 1 monolayer steps. This assignment is further supported by the agreement between the dependence of the experimentally observed peak energies on assigned well thickness and the predictions of the finite square well model, as illustrated in Fig. 2. The dependence of emission energy on well thickness for the structures was calculated[23] using a standard finite square

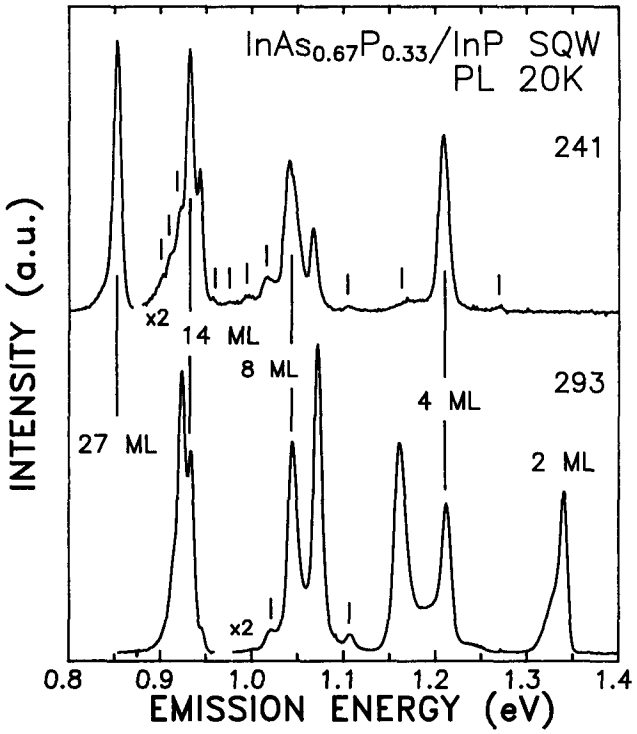

Fig. 1 — 20 K photoluminescence (PL) spectra from two $InAs_xP_{1-x}$/InP strained quantum well structures used for this work. The peak splitting is attributed to emission from regions in the well exhibiting atomically smooth interfaces, separated by one-monolayer steps.

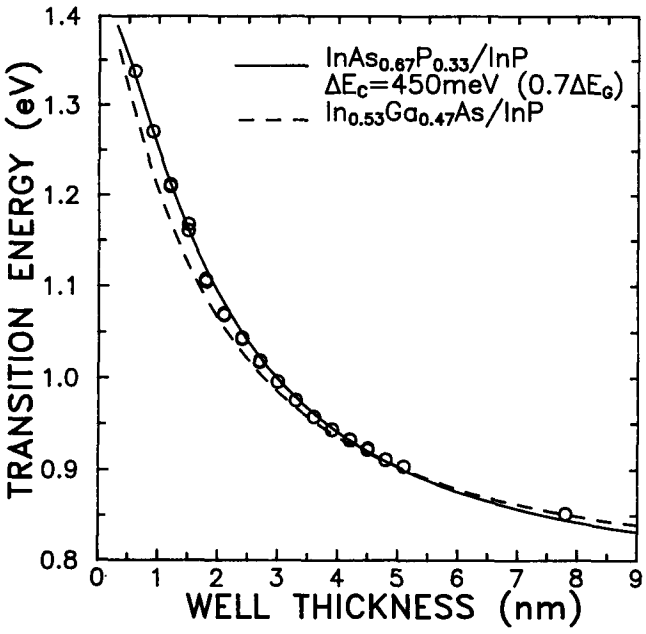

Fig. 2 — Comparison of the experimentally observed dependence of emission energy on well thickness with that predicted by the finite square well model, taking into account the efffects of strain. Also shown is the calculated curve for lattice-matched $In_{0.53}Ga_{0.47}As$/InP QWs.

well model, taking into account the effects of strain.[24,25] Band nonparabolicities and the effect of strain on the effective masses[11,18] were not included in the calculations, however these effects are expected to be small, particularly for the $n = 1$ transitions.[23] The material parameters used for the calculations, including effective masses and deformation potentials, are given in Table I. The strained conduction band offset yielding the best fit to the data was $\Delta E_C = 0.7\Delta E_G$.

For comparison, shown in Fig. 2 is the calculated dependence of emission energy on well thickness for the lattice-matched $In_{0.53}Ga_{0.47}As$/InP QW system, consistent with the results of others.[18] The material parameters used for this calculation are also given in Table I. As shown in Fig. 2 and in Table I, the dependence of emission energy on well thickness for strained $InAs_{0.67}P_{0.33}$/InP and lattice-matched $In_{0.53}Ga_{0.47}As$/InP is very similar, as are the material parameters for the two well compositions.

A typical PLE spectrum obtained from a 4.5 nm-thick $InAs_{0.67}P_{0.33}$/InP strained single quantum well (from sample 293, grown with four wells) is shown in Fig. 3. Also shown in the figure is the PL spectrum for the sample, indicating the PL emission from each of the four wells in the structure. Several features are observed in the spectra. The lowest energy transition at 0.95 eV is the $n = 1$ electron to heavy-hole (E1H1) transition, and is shifted about 15 meV higher in energy than the corresponding PL transition. The feature about 110 meV higher in energy at 1.06 eV is attributed to the $n = 1$ electron to light-hole transition (E1L1). The higher energy transitions, at 1.08 eV and 1.20 eV, are more difficult to identify, and will be discussed in more detail later in this paper. The 1.38 eV transition corresponds to the onset of absorption by acceptor impurities in the InP, and the sharp peak at 1.42 eV is the InP near-band-edge absorption. The observed PLE spectrum is very similar to those obtained from lattice-matched and strained InGaAs(P)/InP quantum well structures using a similar halogen lamp-spectrometer setup for the excitation source.[11,17–19]

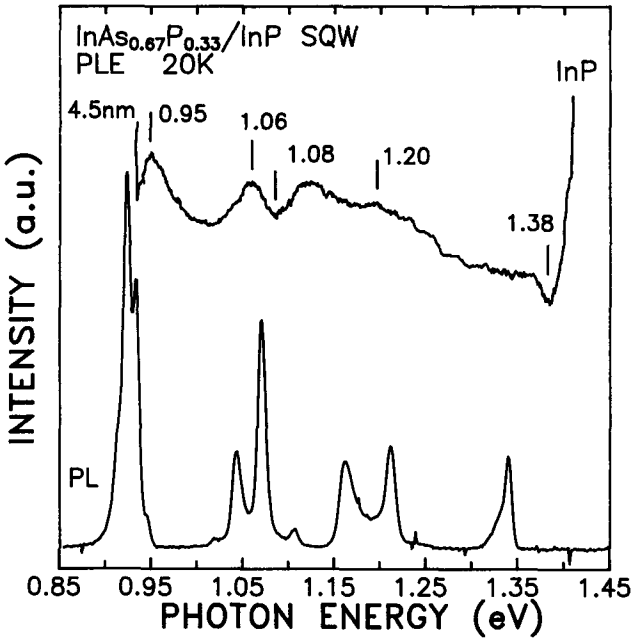

Fig. 3 — 20 K PLE spectrum obtained from a 4.5 nm-thick $InAs_xP_{1-x}$/InP quantum well, shown along with the PL spectrum. Several transitions are observed, as noted in the figure.

The observed shift between the PL peak energy and the E1H1 peak in this PLE spectrum is quite large. In all of the spectra obtained, this shift was on the order of 15–35 meV, and tended to increase with decreasing well thickness. The dependence of this shift (E1H1-PL) on well thickness for all of the samples investigated for this work is given in Fig. 4. Also shown in this figure are the reported values for InGaAs(P)/InP quantum well structures grown by OMVPE and chemical beam epitaxy (CBE), taken from several sources.[16–19] The shifts observed in the present study are consistent with the previous observations for InGaAs/InP QWs.

These large shifts have been previously attributed to a Stoke's shift of the emission.[18] Skolnick *et al.*[16] observed a 28 meV shift between the PL and PL excitation E1H1 peaks for a 11 nm-thick InGaAs/InP quantum well, and based on comparison with the photoconductivity from different sample structures, attributed the large shift to a Moss-Burstein shift. Recently these large shifts have been attributed to binding of the excitons to impurities[17] or potential fluctuations in the well.[19] The observed increase in the binding energy with decreasing well thickness is consistent with both of the latter explanations.[28,29] Evidence for the presence of impurities in these samples has been obtained from studies of the dependence of the PL intensity and lineshape on excitation intensity.[23] Such impurities

Table I. Material parameters used for the calculation of the strain- and quantum-size shifts in $InAs_{0.67}P_{0.33}$/InP and $In_{0.53}Ga_{0.47}As$/InP quantum wells. The InAsP values were linearly interpolated between the reported values for the binary compounds.[26,27] Definitions not given in text: dE_G^o/dP = pressure dependence of band gap (hydrostatic); b = shear deformation potential; Δ_{SO} = spin-orbit band splitting; c_{11}, c_{12} = material elastic constants; a_o = lattice parameter.

	$InAs_{0.67}P_{0.33}$/InP	$In_{0.53}Ga_{0.47}As$/InP
E_G (eV)	0.772 (strained)	0.783
ΔE_C (eV)	0.450 ($0.7\Delta E_G$)	0.316
ΔE_{HH} (eV)	0.193	0.316
m_e^*	$0.041m_o$	$0.041m_o$
m_{hh}^*	$0.68m_o$	$0.52m_o$
m_{lh}^*	$0.048m_o$	$0.056m_o$
dE_G^o/dP (eV/dyne-cm^2)	9.5×10^{-12}	
b (eV)	−1.9	
Δ_{SO} (eV)	0.29	
c_{11} (dyne/cm^2)	8.9×10^{11}	
c_{12} (dyne/cm^2)	4.9×10^{11}	
a_o (nm)	0.59958	0.58686

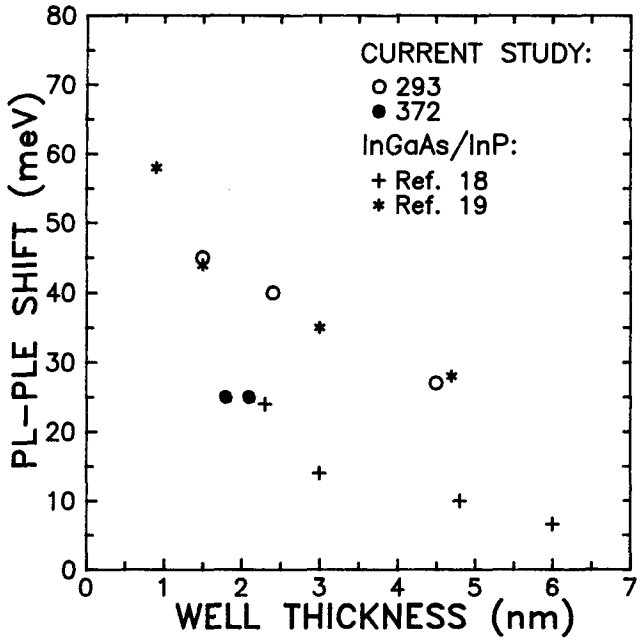

Fig. 4 — The dependence of the observed shift between the PL and the PLE E1H1 transition, PL-E1H1, on well thickness for the $InAs_xP_{1-x}$/InP QWs prepared for this work. Also shown are the typical results obtained for lattice-matched InGaAs/InP QWs.

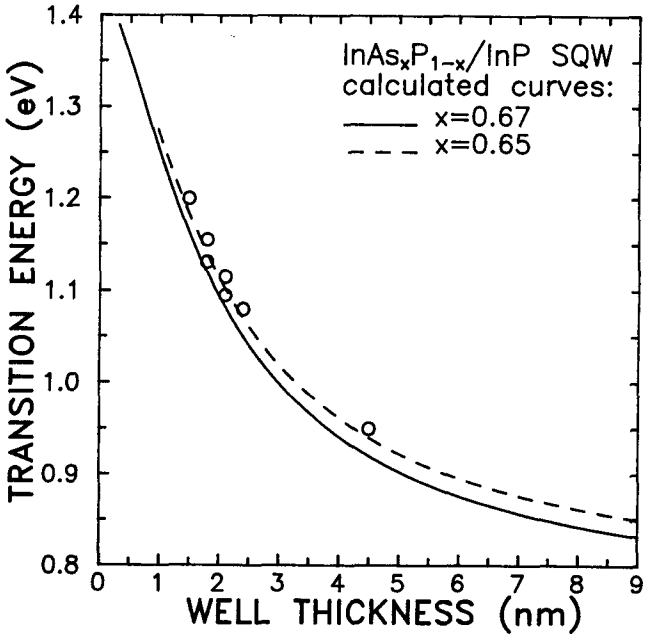

Fig. 5 — The dependence of emission energy on well thickness, calculated using the square well model and taking into account the effects of strain, for $InAs_xP_{1-x}$ QW compositions of $x = 0.65$ and 0.67. Also shown is the experimentally observed dependence of the E1H1 transition energy on well thickness, obtained from the PLE spectra of several samples.

are presumably incorporated during the interruption period during the growth of these samples. However, potential fluctuations, which may take the form of composition fluctuations or interface roughness, are not expected in these samples, which exhibit atomically smooth interfaces.

An important consequence of the observed E1H1-PL energy shift is the effect on the well composition determination. The additional binding energy influences the PL emission energy measured for the thick well, which was used to calibrate the composition of all of the wells. Clearly, a better calibration of the composition is to use the PLE peak energy rather than the PL energy. Shown in Fig. 5 is the dependence of emission energy on well thickness, calculated using the square well model and taking into account the effects of strain, for $InAs_xP_{1-x}$QW compositions of $x = 0.65$ and 0.67. Also shown in the figure is the experimentally observed dependence of the E1H1 transition energy on well thickness, obtained from the PLE spectra of several samples. The lower composition yields better agreement with the data, and will be used for the remainder of the analysis in this paper. Uncertainty in the composition is estimated to be ± 0.01.

For a positive identification of the light hole transitions, it is better to compare the PLE spectra from quantum wells with a range of thicknesses. Shown in Fig. 6 are the PLE spectra obtained from 3 different quantum wells in sample 293, of thickness 4.5 nm (15 ML), 2.4 nm (8 ML) and 1.5 nm (5 ML). Also shown in the figure is the PL spectrum from this sample, with arrows indicating the three PL peaks at which the detection energy was set. The spectrum for the 5 ML well is the same as that shown

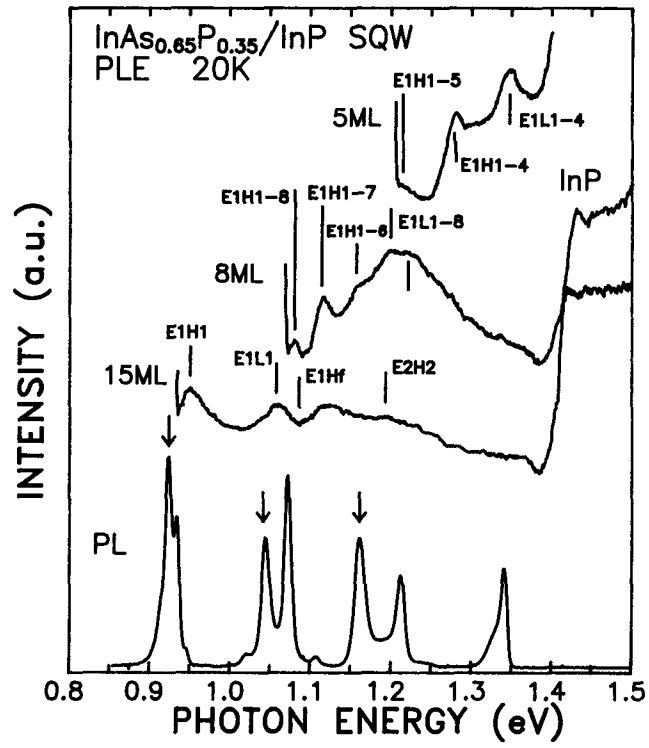

Fig. 6 — 20 K PLE spectra obtained from 3 different quantum wells in sample 293, of thickness 4.5 nm (15 ML), 2.4 nm (8 ML) and 1.5 nm (5 ML). Also shown is the PL spectrum from this sample, with arrows indicating the three PL peaks at which the detection energy was set.

in Fig. 3. In the spectrum from the 8 ML well, four distinct peaks are apparent, labelled E1H1(8), E1H1(7), E1H1(6) and E1L1(8). The lowest energy peak at 1.08 eV is attributed to the E1H1 transition in 8 nm-thick regions in the well. The sharp peak about 30 meV higher in energy at 1.11 eV is too close to the heavy-hole transition to represent the light-hole peak, according to the results of the square well calculations. However this energy spacing is very similar to the spacing between the 8 ML and 7 ML peaks in the PL spectrum. On the basis of this observation we attribute the 1.11 eV peak to excitons which have diffused from the 7 ML-thick (higher energy) regions in the well. Diffusion of excitons from narrower to wider regions in quantum wells has been previously observed in GaAs/AlGaAs quantum wells.[20,30] A third peak at an even higher energy, 1.16 eV, is attributed to diffusion of excitons from regions in the well which are still thinner (6 ML). The two broad features observed at higher energies are then attributed to light-hole transitions in regions in the well which are 8 and 7 ML thick, respectively. The LH transition from 6 ML-thick regions in the well is obscured due to peak broadening. Higher-order transitions (such as $n = 2$ transitions) are not expected in such a thin well.

The transitions observed in the 4 ML-thick well, also shown in Fig. 6, were assigned in a similar manner. Shown in Fig. 7 are the PLE spectra obtained from two very thin wells; sample 372, for which PL peaks attributed to 6 and 7 ML-thick regions in the well were observed, and the 5 ML-thick well in sample 293, shown previously. Distinct peaks are observed in this spectrum and are attributed to heavy- and light hole transitions as noted.

The calculated energy splitting between the light hole and heavy hole transitions in these quantum wells is sensitive to the magnitude of the band offsets. Shown in Fig. 8 is the calculated dependence of the heavy hole-light hole splitting on the well thickness for a well composition of $x = 0.65$ and conduction band offsets of 0.5, 0.6 and $0.75\Delta E_G$. For calculation of the light-hole transitions, the interaction between the spin-orbit split-off band and the light-hole band were taken into account. The two smaller offsets are similar to those used typically for the lattice-matched InGaAs/InP QW structures. Also shown in the figure are the observed energy splittings taken from the PLE spectra. The best agreement between experiment and theory is observed for $\Delta E_C = 0.75\Delta E_G$, or 470 meV. The reduction in the HH-LH splitting in the thin-well regime, predicted by the model and observed experimentally, is simply a consequence of the saturation of the light hole energies at the "top" of the relatively shallow light hole well. In the highly strained InAsP QWs used for the present study, large strain-induced HH-LH splitting contributes to the saturation of the light hole energy in thicker wells (>2 nm thick).

Using the conduction band offset of $0.75\Delta E_G$ obtained from the dependence of the HH-LH splitting on the well thickness, the dependence of the HH and LH transition energies on well thickness was calculated. The results of the calculation are compared to the observed dependence in Fig. 9. In all cases

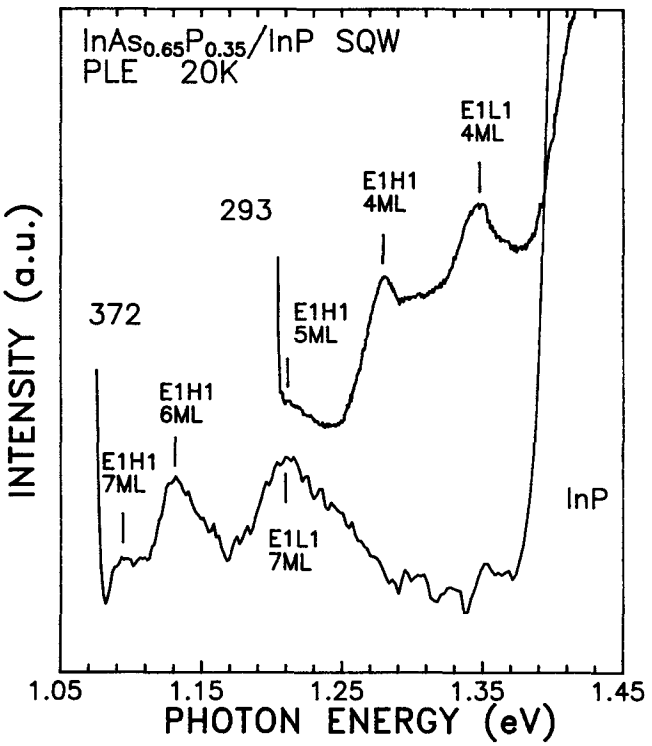

Fig. 7 — 20 K PLE spectra obtained from two very thin wells; sample 372, for which PL peaks attributed to 6 and 7 ML-thick regions in the well were observed, and the 5 ML-thick well in sample 293.

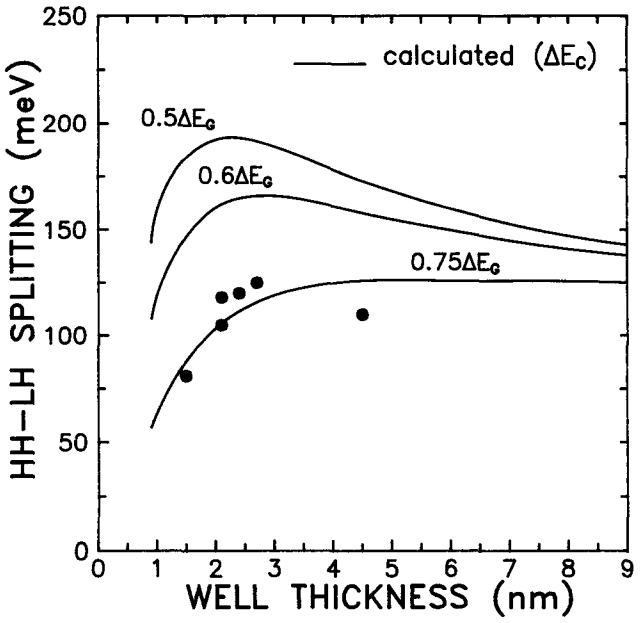

Fig. 8 — The calculated dependence of the heavy hole-light hole splitting on the well thickness for a well composition of $x = 0.65$ and conduction band offsets of 0.5, 0.6 and $0.75\Delta E_G$. Also shown in the figure are the observed energy splittings taken from the PLE spectra.

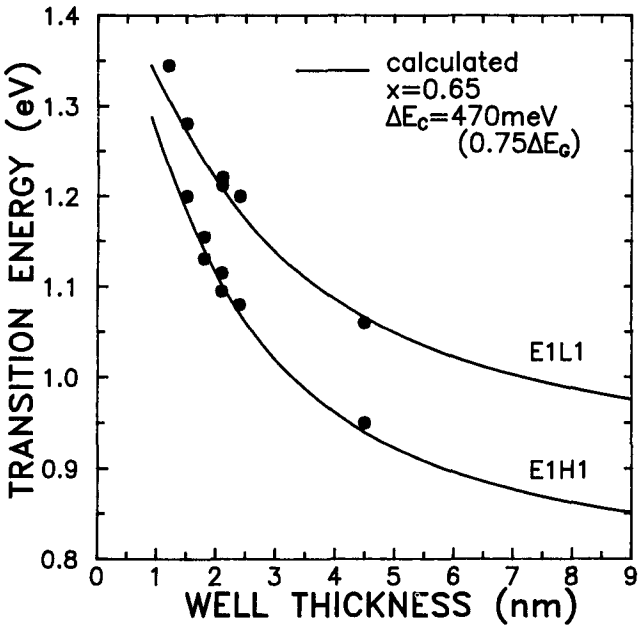

Fig. 9 — Comparison of the dependence of the energy of the observed HH and LH transitions on the well thickness with the calculated results, using a conduction band offset of $0.75\Delta E_G$.

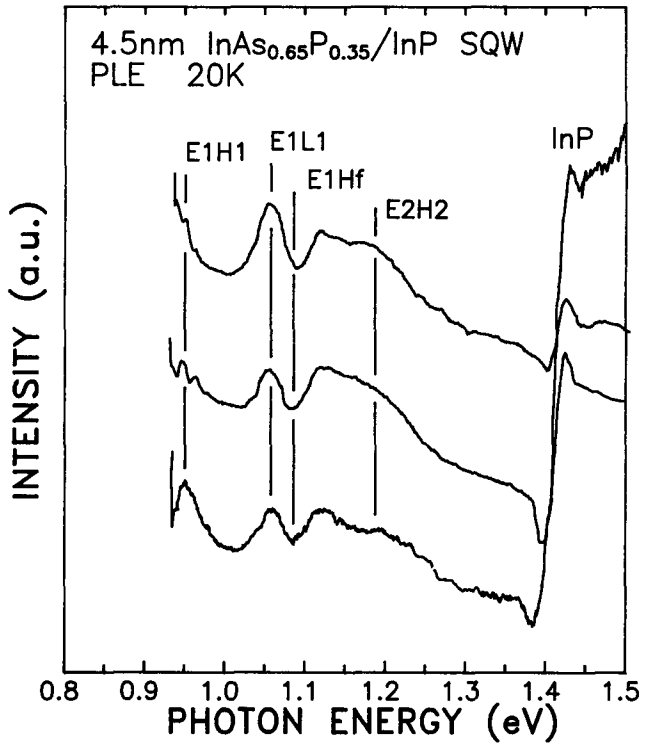

Fig. 10 — PLE spectra obtained from 4.5 · nm thick $InAs_{0.67}P_{0.33}$/InP quantum well structures, including the 4.5 · nm well from sample 293. In all of the spectra the E1H1 and E1L1 transitions are clearly visible, as are two higher-energy transitions, denoted E1Hf and E2H2.

the observed transitions are in good agreement with the theoretical model. This agreement lends strong support to the PLE peak assignment as well as the choice of conduction band offset of 470 meV ($0.75\Delta E_G$). This value is consistent with recent studies. Huang and Wessels[31] extrapolated a conduction band offset of $0.66\Delta E_G$ for this system from transition metal doping studies of unstrained InAsP/InP layers. Waldrop *et al.*[32] reported a conduction band offset of $0.70\Delta E_G$ for InAs/InP single layers, measured using photoemission spectroscopy on unstrained layers.

For wells of thickness greater than about 4 nm, the calculated HH-LH splitting for the InAsP wells is significantly greater than that calculated for lattice-matched InGaAs QWs. In the thin-well regime, the effects of quantum confinement are dominant, and the behavior of both structures is very similar. Greatest HH-LH splitting is obtained in the thicker $InAs_{0.65}P_{0.35}$/InP strained QWs (QW thicknesses as great as ~8 nm are feasible for this composition).

According to the square well calculations, the n = 2 E-HH (E2H2) transitions are confined in $InAs_{0.65}P_{0.35}$/InP quantum wells for well thicknesses greater than about 4 · nm (the E2L2 transitions are confined only for much thicker layers). Shown in Fig. 10 are PLE spectra obtained from 4.5 · nm thick $InAs_{0.65}P_{0.33}$/InP quantum well structures, including the 4.5 · nm well from sample 293. In all of the spectra the E1H1 and E1L1 transitions are clearly visible, as are two higher-energy transitions, denoted E1Hf and E2H2.

The highest energy peak is attributed to transitions between the n = 2 electrons and n = 2 heavy holes, E2H2. The square well model overestimates the energy of the observed n = 2 transition by 50–80 meV. An additional source of uncertainty in calculating these higher-order transitions, however, is the carrier effective mass. Recent reports have shown that the higher-order transitions can be fit to theoretical models only when band nonparabolicities are taken into account.[18,19] Taking such nonparabolicites into account would result in a reduction of the predicted transition energy, which would yield better agreement with the experimentally observed transition. Because of the inherent uncertainty in determining effective mass values, however, the higher-order transitions are not as sensitive a measure of the band offset as is the HH-LH splitting.

According to the calculations, the transition about 100 meV lower in energy than the E2H2 cannot be due to parity-allowed confined state transitions. In addition, the E1H2 transition is not expected to be at such high energies. In recent spectroscopic investigations (both photoluminescence excitation and photocurrent) of lattice-matched InGaAs(P)/InP SQW structures, transitions have been noted which are attributed to "free"-(unbound-) to confined-carrier transitions, *e.g.*, between "free" electrons at the top of the well and heavy holes confined in the well (EfH1),[16,33] or alternatively, between confined electrons and free heavy holes at the "top" of the heavy hole well (E1Hf).[17,33] Positively identified, these transitions may provide the most direct measurement of the magnitude of the band offsets. This is because the uncertainty in the measurement is influenced only by the uncertainty in the calculated electron or hole subband shifts, which are weakly dependent on the value of the band offset.

As shown in Fig. 10, the PLE peaks observed in

all three samples at about 1.08 eV are attributed to the E1Hf transition. The transitions are marked according to the onset rather than a peak because the transition is between a confined state and a band, rather than between two discrete confined states. Using the strained bandgap of 0.792 eV and a calculated electron subband shift of 130 meV for a 4.5 nm-thick well, the valence band offset is measured as 1.08 − 0.79 − 0.13 = 0.16 eV. This is equivalent to a conduction band offset of 460 meV ($0.74\Delta E_G$), in good agreement with the previous assignment of 470 meV ($0.75\Delta E_G$), and offers additional support for this value of band offset.

CONCLUSIONS

In summary, we have used photoluminescence excitation spectroscopy to evaluate the optical emission characteristics of strained $InAs_{0.65}P_{0.35}$/InP quantum wells. Distinct features attributed to n = 1 heavy-hole (E1H1) and light-hole (E1L1) transitions were observed, as well as higher-energy transitions attributed to transitions involving n = 2 electrons and heavy holes (E2H2), and n = 1 bound electrons and "unconfined" holes (E1Hf). The E1H1-E1L1 transition energy difference was a sensitive measure of the band offset. Comparison of the observed dependence of the splitting on well thickness to that calculated using a square-well model, taking into account the effects of strain, yielded a conduction band offset of $\Delta E_C = 0.75\Delta E_G$. Using this offset, good agreement between the observed E1H1 and E1L1 transition energies and those predicted by the square-well model was noted. The energy position of the E1Hf transition is consistent with this band offset. The optical emission characteristics of these strained InAsP/InP quantum wells were found to be similar to those of the lattice-matched InGaAs/InP QWs. Important differences in the InAsP system include a larger ΔE_C, larger HH-LH splitting in thicker (>4 nm) QWs, and large (~2.1%) biaxial compressive strain. Thus, the InAsP/InP strained-layer materials system is well suited for optoelectronic device application in the 1.3–1.6 μm wavelength range, and may exhibit significant advantages to lattice-matched InGaAs(P)/InP.

ACKNOWLEDGMENTS

This work was supported by the National Science Foundation through Northwestern University Materials Research Center, Grant No. DMR 85-20280.

REFERENCES

1. W. Stutius, P. Gavrilovic, J. E. Williams, K. Meehan and J. Zarrabi, Electron. Lett. *24,* 1493 (1988).
2. P. J. A. Thijs, E. A. Montie, T. van Dongen and C. W. T. Bulle-Lieuwma, presented at ICCBE 2, Houston, 1989; to be published in J. Cryst. Growth.
3. M. C. Wu, N. A. Olsson, D. Sivco and A. Y. Cho, Appl. Phys. Lett. *56,* 221 (1990).
4. T. Tanbun-Ek, R. A. Logan, N. A. Olsson, H. Temkin, A. M. Sergent, and K. W. Wecht, Appl. Phys. Lett. *52,* 224 (1990).
5. G. C. Osbourn, Mat. Res. Soc. Symp. Proc. *37,* 219 (1985); J. Vac. Sci. Technol. *A3,* 826 (1985).
6. E. P. O'Reilly and G. P. Witchlow, Solid State Commun. *62,* 653 (1987).
7. E. Yablanovitch and E. O. Kane, IEEE J. Lightwave Technol. *LT-6,* 1292 (1988).
8. E. P. O'Reilly, Semicond. Sci. Technol. *4,* 121 (1989).
9. M. H. Meynadier, J.-L. de Miguel, M. C. Tamargo and R. E. Nahory, Appl. Phys. Lett. *52,* 302 (1988).
10. J. L. de Miguel, M. C. Tamargo, M.-H. Meynadier, R. E. Nahory and D. M. Hwang, Appl. Phys. Lett. *52,* 892 (1988).
11. D. Gershoni, H. Temkin, M. B. Panish and R. A. Hamm, Phys. Rev. *B39,* 5531 (1989).
12. R. P. Schneider, Jr. and B. W. Wessels, TMS-Electron. Mater. Conf., Cambridge, MA (1989).
13. R. P. Schneider, Jr. and B. W. Wessels, Appl. Phys. Lett. *54,* 1142 (1989).
14. R. P. Schneider, Jr. and B. W. Wessels, Mater. Res. Soc. Symp. Proc. *145,* 145 (1989).
15. R. P. Schneider, Jr. and B. W. Wessels, TMS-Electron. Mater. Conf., Santa Barbara, CA (1990).
16. M. S. Skolnick, P. R. Tapster, S. J. Bass, A. D. Pitt, N. Apsley and S. P. Aldred, Semicond. Sci. Technol. *1,* 29 (1986).
17. E. A. Montie, P. J. A. Thijs and G. W. 't Hooft, Appl. Phys. Lett. *53,* 1611 (1989).
18. R. Sauer, T. D. Harris and W. T. Tsang, Phys. Rev. *B34,* 9023 (1986).
19. D. Gershoni, H. Temkin and M. B. Panish, Phys. Rev. *B38,* 7870 (1988).
20. R. C. Miller, C. W. Tu, S. K. Sputz and R. F. Kopf, Appl. Phys. Lett. *49,* 1245 (1986).
21. P. L. Gourley and R. M. Biefeld, Appl. Phys. Lett. *45,* 749 (1984).
22. D. Gershoni, J. M. Vandenberg, S. N. G. Chu, H. Temkin, T. Tanbun-Ek and R. A. Logan, Phys. Rev. *B40,* 10017 (1989).
23. R. P. Schneider, Jr., Ph.D. thesis, Northwestern University (1989).
24. H. Asai and K. Oe, J. Appl. Phys. *54,* 2052 (1983).
25. G. Ji, D. Huang, U. K. Reddy, T. S. Henderson, R. Houdre' and H. Morkoc, J. Appl. Phys. *62,* 3366 (1987).
26. S. Adachi, J. Appl. Phys. *53,* 8775 (1982).
27. Landolt-Bornstein New Series (1982).
28. G. Bastard, Phys. Rev. *B24,* 4714 (1981).
29. R. C. Miller, D. A. Kleinman, A. C. Gossard and O. Monteanu, Phys. Rev. *B25,* 6545 (1982).
30. D. C. Reynolds, K. K. Bajaj, C. W. Litton, J. Singh, P. W. Yu, P. Pearah, J. Klem and H. Morcoc, Phys. Rev. *B33,* 5931 (1986).
31. K. H. Huang and B. W. Wessels, Appl. Phys. Lett. *52,* 1155 (1988).
32. J. R. Waldrop, R. W. Grant and E. A. Kraut, Appl. Phys. Lett *54,* 1878 (1989).
33. M. Zachau, P. Helgeses, F. Koch, D. Grutzmacher, R. Meyer and P. Balk, Semicond. Sci. Technol. *3,* 1029 (1988).